Journal of Engineering and Applied Science

RESEARCH Open Access

Hybrid air conditioning and seawater desalination system assisted by solar energy: thermoeconomic investigation and optimization

Nashwa Yosry[1], Essam Elgendy[2*], Ahmed Mostafa[1,3] and Mohamed Fatouh[1]

*Correspondence:
elgenady@aast.edu

[1] Mechanical Power Engineering Department, Faculty of Engineering at El-Mattaria, Helwan University, Cairo, Egypt
[2] Mechanical Engineering Department, College of Engineering & Technology at Arab Academy for Science, Technology & Maritime Transport, Cairo, Sheraton, Egypt
[3] Energy and Renewable Energy Engineering Program, Faculty of Engineering and Technology, Egyptian Chinese University, Ain Shams, Egypt

Abstract

The demand for freshwater has become progressively critical due to population growth and water scarcity. The current work investigates the energetic performance of a hybrid absorption refrigeration and desalination system. A parametric study for the system operating conditions has been performed to get the optimal conditions. Also, economic analysis and a multi-objective optimization method are used with the aim of maximizing the energy utilization factor of the system and minimizing total costs. The specific cost of desalinated water from the multi-objective optimization is calculated as (1.728 Cent/L) with the greatest energy utilization factor of (2.214). It turns out that, the system performs optimum at condensation and generation temperatures of 30 and 65 °C respectively, with resultant COP and GOR of 0.84 and 1.37. Using the optimum conditions, TRNSYS has been used to investigate the transient performance of the system for Marsa–Matrouh City in Egypt. The cooling and freshwater demands are 10 kW and 24 L/h. It was concluded that the input energy required to run the hybrid system decreased by about 65% less than that required for separate systems. With the assistance of solar energy, it became clear that the energy required was 60% less than the hybrid system as well.

Keywords: Hybrid systems, Absorption, Seawater desalination, HDH system, Solar energy

Introduction

Energy is the driving force behind several applied functions, including water purification, transportation, mobility, homes, communication systems, and other applications [1]. In 2022, the global energy consumption for industry, buildings, and transport was 37.8%, 30%, and 26.2% respectively [2]. Air conditioning represents one of the most important applications in the industrial sector and contributes nearly 38.9% of the total electricity demand in buildings [3]. On the other hand, water shortage is a real and serious crisis [4]. Nearly 700 million people suffer from drinkable water availability [5]. Global water resources are predicted to be roughly 40% less by 2030 than the necessary

amount needed to meet demand [6]. As the global population continuously grows, the demand for air conditioning (AC) and water also increases.

Many ideas and concepts have been developed by researchers for the combination of cogeneration air conditioning and water desalination systems. The integrated systems offer a higher energy utilization factor (EUF) and can serve as a substitute approach to fulfill the needs for air conditioning and water in the world [7]. Humidification and humidification desalination (HDH) is considered one of the most effective water desalination techniques due to its simplicity, low cost, and utilization of low-grade energy [8]. Therefore, many investigators focused on the integration between HDH desalination and AC systems [9]. Nada et al. [10] investigated an experimental study of a hybrid vapor compression refrigeration system integrated with HDH water desalination. The proposed system consists of four independent main loops (refrigerant, humid air, fresh water, and sea water loops). They studied the influences of system operating parameters (air mass flow rate, air inlet temperature, air inlet specific humidity, and the evaporator saturation temperature) on desalinated water production rate, evaporator refrigeration capacity, compressor work per kilogram of fresh water, mass transfer coefficient and conditioned space-supplied air conditions (air temperature and relative humidity). The system could generate an integrated cooling capacity of 146.7 kWh and a maximum daily freshwater productivity of 501 kg. The results show the enhancement of the freshwater production rate, the refrigeration capacity, and the compressor work per kilogram of fresh water with increasing air-specific humidity and air mass flow rate.

He et al. [11] proposed and analyzed an HDH system operated by a mechanical vapor compression system, with the condenser to heat the preheated seawater and evaporator to recover the internal energy of the discharged hot brine. Results showed that the compression pressure ratio directly relates to the amount of water produced. Moreover, the price of gained water is 0.018$/L. Abdelgaied et al. [12] investigated the performance of a solar-assisted integrated HDH with desiccant AC system. It was concluded that by changing the regeneration air temperature within range (75 to 95 °C), the distillation water productivity increased by 58% while the overall COP decreased by 20%. Wang et al. [13] studied another configuration of a desiccant air conditioning system coupled with a HDH unit. In their configuration, the evaporator has been used for dehumidification while the condenser acted as the preheated in the HDH system. The cooling system COP was 0.411 for an air mass of 0.78 kg/s and the best value for distillate water was 4.9 L/h, he maximum electrical power generation capacity and electrical efficiency of the photovoltaic collector were obtained at 0.72 kWh, and 13.7%, respectively.

The first integrated HDH and absorption cooling system has been investigated by Chiranjeevi and Srinivas [7]. The double-stage HDH desalination unit has been combined with a single-stage absorption refrigeration system. Ammonia-water solution pair was used as a working fluid in the absorption system. The generator heat load is 200 kW with a hot fluid temperature of 127 °C. The integrated plant aimed to produce fresh water and a cooling capacity of 670 L/h and 75 kW, respectively. Two heat sources have been utilized for the plant operation one for the cooling cycle and the other for the desalination unit. The system EUF for the plant was 0.33. Following this work, Bhowmick and Kundu [14] studied a combined absorption and HDH desalination system. In their study, the released heat from the absorption system has been used to desalinate the seawater

of the HDH system. The reported results revealed that the generation temperature to drive the system ranged from 122 to 150 °C. Following the previous publication, Beniwal et al. [15] presented a novel combination of an absorption heat transformer, an absorption refrigeration system, and an HDH desalination system. This system will not only provide refrigeration (between − 5 °C to − 15°C) with the help of waste heat at a temperature of 90 °C, which will be helpful in the storage of highly perishable medicine and frozen foodstuff but will also provide fresh water. The system reported 70kW of refrigeration effect is provided with 20 kg/h of distillate production rate. An exergy destruction of 82.64 kW has been reported for a total input exergy of 142.2 kW, for a refrigeration capacity of 157 kW. Recently, Elgendy [16] investigated the energetic performance of a double-effect vapor absorption refrigeration system integrated with an HDH desalination system using H2O–LiCl. The system driving temperature could be lowered by 4 °C and 9 °C using H2O–LiCl than H2O–LiBr at condensation temperatures of 30 °C and 40 °C, respectively.

Considering the previously mentioned literature, all investigations have been focused on analyzing the performance of the integrated air conditioning–HDH system using vapor compression, desiccant or absorption system. However, vapor compression systems were driven by high-grade energy sources (electric energy) and desiccant systems had the lowest COP. The heat generation temperature for the double-effect absorption system was very high (> 100 °C). Therefore, the present study aims to optimize an integrated air conditioning and HDH system driven by low-generation temperature. A single-effect vapor absorption system is used for air conditioning purposes while HDH is used for water desalination. A detailed parametric study by varying evaporation, condensation, and generation temperatures has been applied. Then, a multi-objective optimization of the integrated plant based on energy utilization and cost has been performed under various operating conditions. Then, the hourly performance of the proposed system driven by solar energy has been introduced under real climatic conditions for certain locations by maintaining the optimum operating conditions.

Methods

Figure 1 displays the proposed SEAC–HDH system which consists of three basic subsystems. The first subsystem is an HDH desalination unit. The second main subsystem used for cooling purposes is a SEAC system. These two subsystems were driven by the third subsystem, the solar field.

The SEAC subsystem includes a generator, condenser, solution heat exchanger, absorber, evaporator, two expansion valves, and a solution pump. The SEAC subsystem operates at two pressure levels (P_{Gen} and P_{Abs}). The high-pressure level (P_{Gen} or P_{Con}) is maintained at state points 2, 3, 4, 5, 7, and 8, and the low-pressure level (P_{Abs} or P_{Eva}) at state points 1, 6, 9, and 10. There are also two levels of solution concentrations (in terms of LiBr concentration): strong and weak concentration.

The weak solution concentration is maintained at state points 1, 2, and 3, while the strong concentration is maintained at state points 4, 5, and 6. The weak solution exiting the absorber (state point 1) is pumped to the generator via the solution heat exchanger (SHE). Water vapor is produced in the generator as a result of the heat input from the sun field, resulting in a strong concentration solution (state point 4). The heat

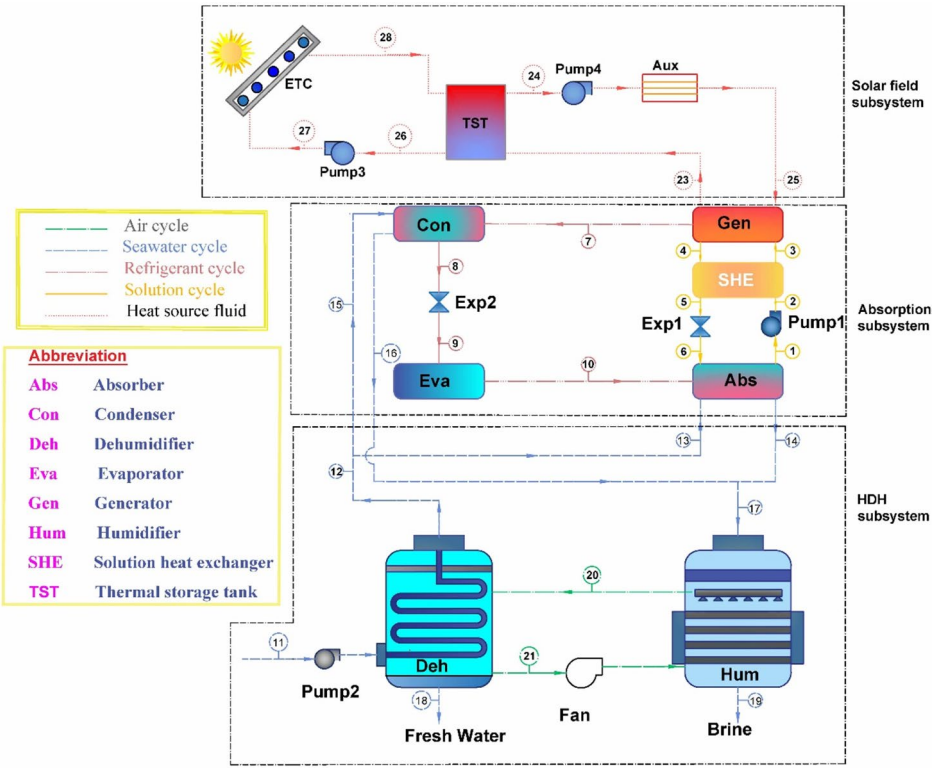

Fig. 1 Schematic diagram of solar-driven SEAC integrated with HDH desalination system

from this solution is transported to the weak solution via the SHE, and finally to the absorber via an expansion valve (Exp1). The created water vapor from the generator (state point 7) enters the condenser and transfers heat to the seawater stream process (15–16). The condensed liquid refrigerant (water) (state point 8) is then routed to the evaporator through the expansion valve (Exp2). The liquid refrigerant is evaporated in the evaporator (state point 10) before being dissolved with the weak solution in the absorber. The heat released in the absorber by the saturated water vapor and the strong solution is transferred to the seawater stream (process 13–14). The HDH subsystem is a closed-air, open-water (water–heated) system. The HDH system's primary components are a humidifier, a dehumidifier, a fan, and a seawater pump, as shown in Fig. 1. This combination maximizes the total utilization of input energy by heating the seawater with heat released by the SEAC subsystem's condenser and absorber rather than from an external source. The seawater is injected into the dehumidifier (state point 11). The saline water temperature rises as it absorbs heat from the hot air in the dehumidifier (process 11–12). Once the humid air has condensed, the freshwater produced by the dehumidifier is collected. After entering the dehumidifier (state 12), the warm seawater flows into the SEAC, where it collects heat from the condenser and absorber. It should be noted that the seawater stream is separated into two streams dependent on the heat emitted by the condenser and absorber. Following heating, a cold air stream from the opposite direction (processes 21–20) is used to spray the hot saline water inside the humidifier (state point 17), and any remaining water that has not evaporated is prevented from use as brine (state point 19).

The solar field subsystem includes an evacuated tube collector (ETC), a thermal storage tank (TST), an auxiliary heater, a generator, and two pumps. The solar collector aperture area is 2.858 m^2, with the thermal storage tank volume calculated as (0.01–0.02) of the solar collector area (Li et al., 2015) [17]. When the thermal storage tank is insufficient to meet the absorption system's energy requirements, an auxiliary heater is needed. Using solar energy as the primary heat source eliminates the need for conventional energy sources while lowering greenhouse gas emissions. Table 1 exhibits the solar collector specifications [18].

Simulation model

Mass and energy balances have been applied to each component of the proposed system. The SEAC is working with H_2O–LiBr solution as the working fluid. The following assumptions have been considered:

- All components of the proposed system run at steady–state conditions.
- All components' heat loss is neglected.
- The pressure drops in all components and in the pipes are ignored.
- Pumping and fan powers are negligible compared to thermal energy input
- The exits of the condenser and evaporator are supposed to be saturated refrigerant.
- In the expansion valves, the throttling process is assumed to be isenthalpic process.
- The condensate water temperature at the exit of the dehumidifier is balanced with the average temperature between the outlet and inlet moist air. [19]
- The salinity of the inlet seawater is 35 g/kg.
- Motor efficiency of the pump is taken as 90% while the SHE efficiency is taken as 70%.
- The relative humidity of the humid air leaves both the humidifier and the dehumidifier are 90% [20]. Engineering equation solver (EES) has been used for solving the equations in steady state mode of operation and TRNSYS software has been used in transient system simulation.

Model of hybrid SEAC–HDH system

The mass and energy balance formulas for each part of the suggested hybrid SEAC–HDH are displayed in Table 2.

Table 1 The solar collector specifications

Parameter	Value
Dimensions (L × W × H)	2 × 2.19 × 0.134 m
Aperture area	2.858 m^2
Gross area	4.397 m^2
Rated flow	113.56 L/h
Intercept efficiency	0.7163
1st order efficiency coefficient	1.257 $W/m^2.K$
2nd order efficiency coefficient	0.0089 $W/m^2.K$

Table 2 Mass and energy equations for the hybrid SEAC–HDH

Component	Mass balance	Energy balance
Generator	$\dot{m}_{25} = \dot{m}_{23}$ $\dot{m}_3 = \dot{m}_4 + \dot{m}_7$	$Q_{Gen} = \dot{m}_{23}(h_{25} - h_{23})$ $Q_{Gen} = \dot{m}_7 h_7 + \dot{m}_4 h_4 - \dot{m}_3 h_3$
SHE	$\dot{m}_4 = \dot{m}_5$ $\dot{m}_2 = \dot{m}_3$	$\dot{m}_4(h_4 - h_5) = \dot{m}_3(h_3 - h_2)$
Exp1	$\dot{m}_6 = \dot{m}_5$	$h_6 = h_5$
Exp2	$\dot{m}_8 = \dot{m}_9$	$h_8 = h_9$
Pump1	$\dot{m}_1 = \dot{m}_2$	$h_1 = h_2$
Condenser	$\dot{m}_7 = \dot{m}_8$ $\dot{m}_{15} = \dot{m}_{16}$	$Q_{Con} = \dot{m}_7(h_7 - h_8)$ $Q_{Con} = \dot{m}_{15}(h_{16} - h_{15})$
Evaporator	$\dot{m}_{10} = \dot{m}_9$	$Q_{Eva} = \dot{m}_9(h_{10} - h_9)$
Absorber	$\dot{m}_1 = \dot{m}_6 + \dot{m}_{10}$ $\dot{m}_{14} = \dot{m}_{13}$	$Q_{Abs} = \dot{m}_{10} h_{10} + \dot{m}_6 h_6 - \dot{m}_1 h_1$ $Q_{Abs} = \dot{m}_{13}(h_{14} - h_{13})$
Dehumidifier	$\dot{m}_{11} = \dot{m}_{12} + \dot{m}_{18}$ $\dot{m}_{20} = \dot{m}_{21}$ $\dot{m}_{18} = \dot{m}_{20}(HR_{21} - HR_{20})$	$\dot{m}_{11} h_{11} + \dot{m}_{20} h_{20} = \dot{m}_{12} h_{12} + \dot{m}_{18} h_{18} + \dot{m}_{21} h_{21}$
Humidifier	$\dot{m}_{20} = \dot{m}_{21}$ $\dot{m}_{19} = \dot{m}_{17} + \dot{m}_{20}(HR_{20} - HR_{21})$	$\dot{m}_{21} h_{21} + \dot{m}_{17} h_{17} = \dot{m}_{20} h_{20} + \dot{m}_{19} h_{19}$
Auxiliary heater	$\dot{m}_{24} = \dot{m}_{25}$	$Q_{Aux} = \dot{m}_{24}(h_{25} - h_{24})$
Solar collector	$\dot{m}_{28} = \dot{m}_{27}$	$Q_{ETC} = \dot{m}_{27}(h_{28} - h_{27})$

The ratio of the dry-air mass flow rate to the water mass flow rate is known as the mass ratio (MR), and it can be stated as follows [21]:

$$\mathrm{MR} = \frac{\dot{m}_w}{\dot{m}_{da}} \tag{1}$$

$$\mathrm{GOR} = \frac{\dot{m}_{fw} h_{fg}}{Q_{Gen}} \tag{2}$$

The HDH system performance is commonly examined by the GOR, which can be expressed as [21]:

$$\mathrm{GOR} = \frac{\dot{m}_{fw} h_{fg}}{Q_{Aux}} \tag{3}$$

where h_{fg} indicates the latent heat of condensation. In the case of solar-assisted HDH system, the GOR can be calculated as [16]:

The hybrid system performance can be characterized by the EUF as follows [22];

$$\mathrm{EUF} = \frac{\dot{m}_{fw} h_{fg} + Q_{Eva}}{Q_{Gen}} \tag{4}$$

In the case of solar-assisted hybrid system, the EUF can be estimated as [16];

$$\mathrm{EUF} = \frac{\dot{m}_{fw} h_{fg} + Q_{Eva}}{Q_{Aux}} \tag{5}$$

Figure 2 illustrates the flow chart for the program constructed using EES while the TRNSYS program used for the solar field subsystem is shown in Fig. 3.

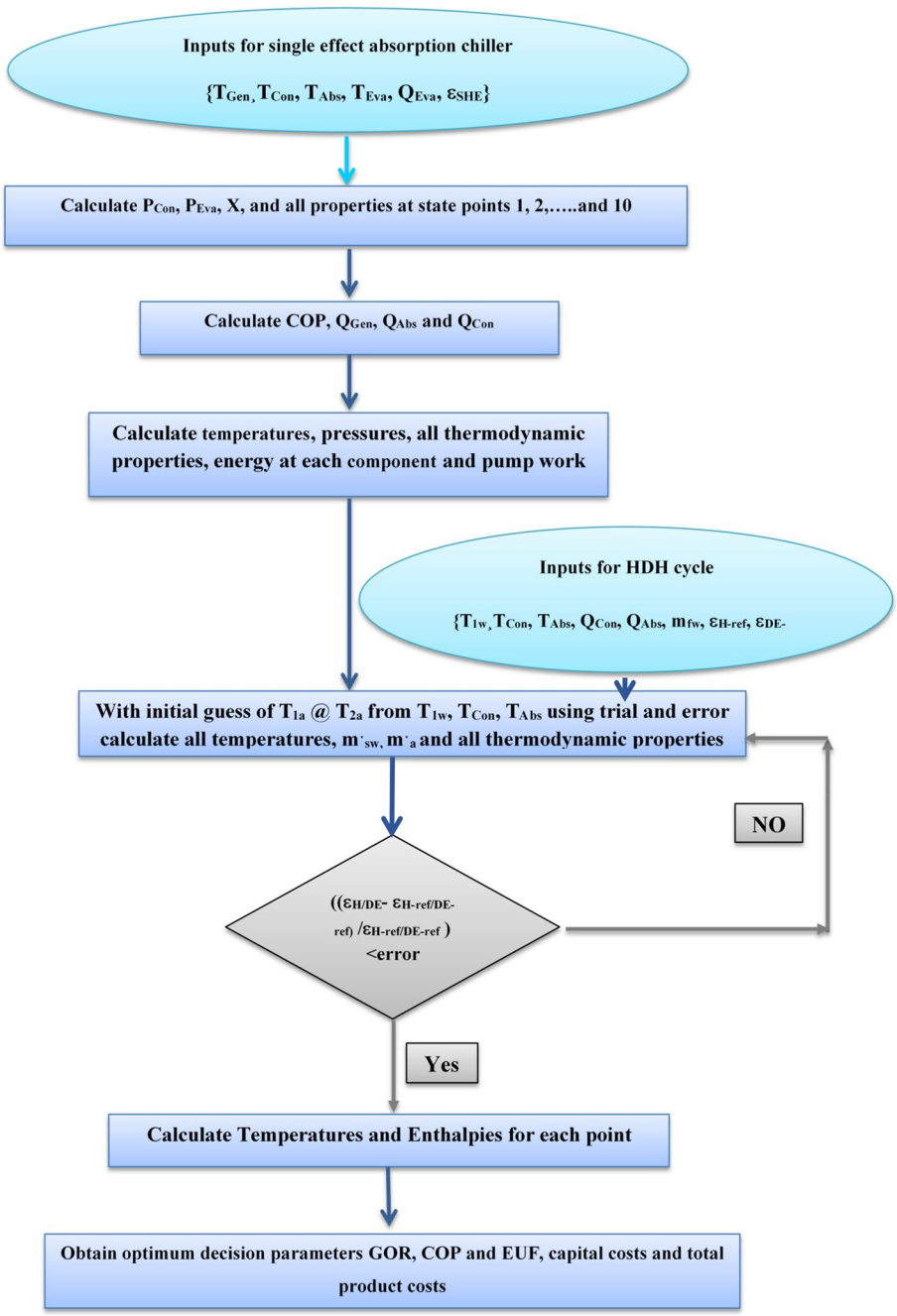

Fig. 2 Flow chart for the simulation program

Results and discussion

In this section, firstly a verification of the present model with the published data will be introduced. Then, a parametric study for the operating system conditions was performed to investigate the steady and transient system performance. An economic study was performed, and multi-objective optimization was investigated. The cooling and freshwater demands are 10 kW and 24 L/h.

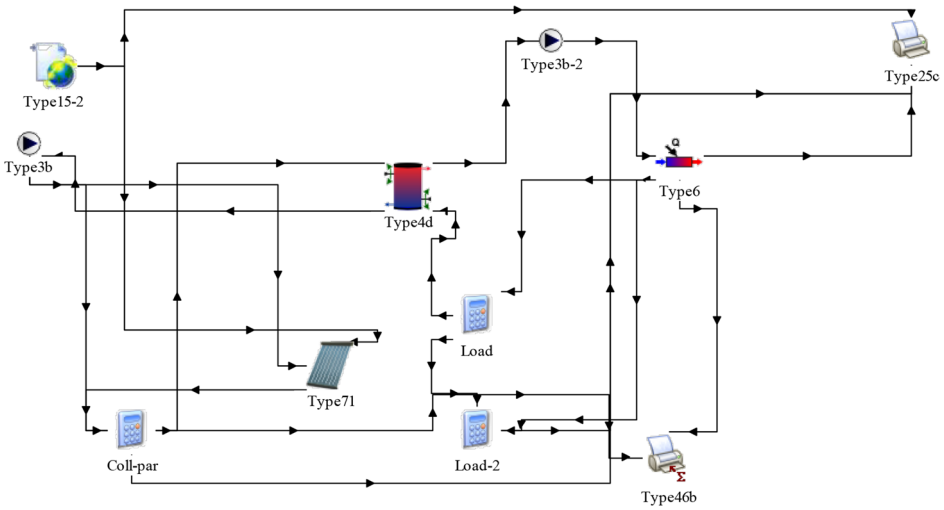

Fig. 3 TRNSYS simulation program

Model verification

The simulation results of SEAC energy analysis of the present model have been compared with the available numerical data reported by Kaushik and Arora [20] and its details are presented in Table 3. A good agreement has been found, with a maximum error percentage of 1.5%.

Figure 4 compares the present simulation model with the theoretical results of Sharqawy et al. [22]. Obviously, the present model GOR has a good agreement with the previous results. The average error percentage is 1.94%.

Steady state hybrid SEAC-HDH system performance

In a hybrid SEAC–HDH system, the system performance indexes (COP, GOR, and EUF) are affected by the generator temperature. Figure 5 depicts how differences in generator temperature effect the COP, GOR, and EUF of hybrid SEAC–HDH at various evaporation temperatures. Higher generator temperatures typically result in higher COP values, which subsequently become nearly constant. This is because a greater generator temperature results in less generator input energy at a constant cooling capacity. Furthermore, the GOR drops as the generator's input energy decreases. The temperature of the generator also has an impact on system EUF; because EUF is essentially the SUM product of COP and GOR, raising the generator temperature usually results in improvement.

Figure 5 shows the impact of varying evaporation temperatures ranging from 4 to 10 °C) at a constant condensation temperature of 35 °C on hybrid system performance indices. Obviously, when the evaporation temperature decreases, so do all of the system performance indicators. As the evaporation temperature drops, the necessary generator input energy rises, and COP, GOR, and EUF fall at constant system cooling capacity and freshwater flow rate. Lowering the evaporator temperature from 10 to 4 °C while maintaining constant condensation and absorption temperatures (Fig. 5) decreases COP, GOR, and EUF values by 6.3%, 59.5%, and 34%, respectively, at the same generator temperature. Furthermore, lowering the evaporator temperature from 10 to 4 °C decreases the optimal generation temperature from 78 to 90 °C.

Table 3 Comparison between the present analysis and Kaushik and Arora [20]

Inputs: ε = 0.7, Q_{Eva} = 354.4 kW, T_{Eva} = 7.2 °C, T_{Con} = 37.8 °C, T_{Abs} = 37.8 °C, T_{Gen} = 87.8 °C				
	COP	**Q_{Abs} (kW)**	**Q_{Con} (kW)**	**Q_{Gen} (kW)**
Kaushik and Arora [20]	0.76	2945	2506	3096
Present work	0.77	2901	2506	3052
Error %	1.19	− 1.5	0.004	− 1.4

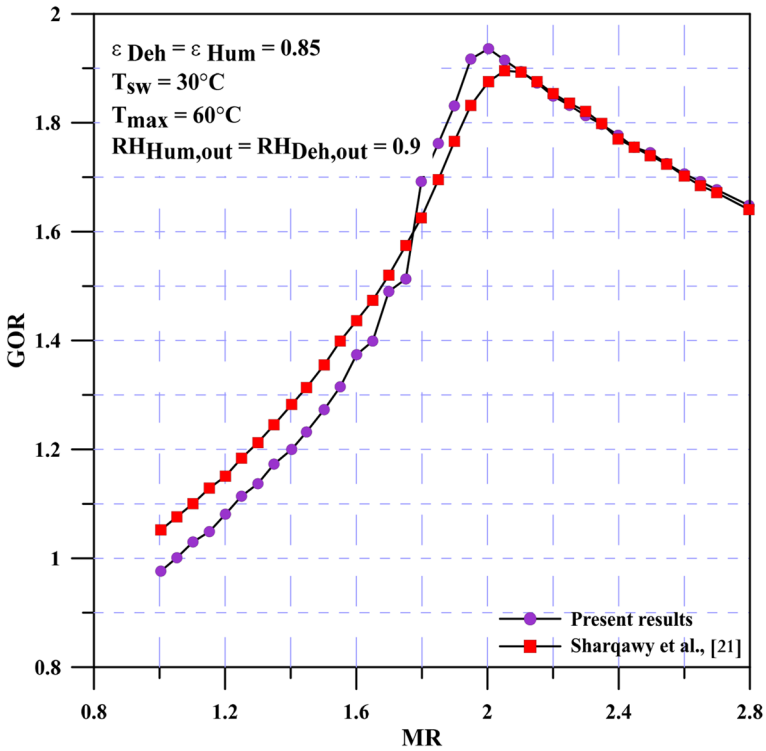

Fig. 4 Simulation model verification with literature data

Figure 6 shows how changing the generator temperature affects the COP, GOR, and EUF of hybrid SEAC-HDH at various condensation temperatures. Lowering the condenser and absorber temperatures while maintaining the evaporator temperature constant may increase the COP.

Changing the condensation temperature from 40 to 30 °C increases COP, GOR, and EUF by 10.4%, 66.3%, and 39.4%, respectively. Lowering condensation temperature from 40 to 30 °C reduces generation temperature by 20 °C.

Economic model

The procedure adopted by this study for estimating the desalinated water cost is presented here. It involves some of the design and operating parameters of the system, as

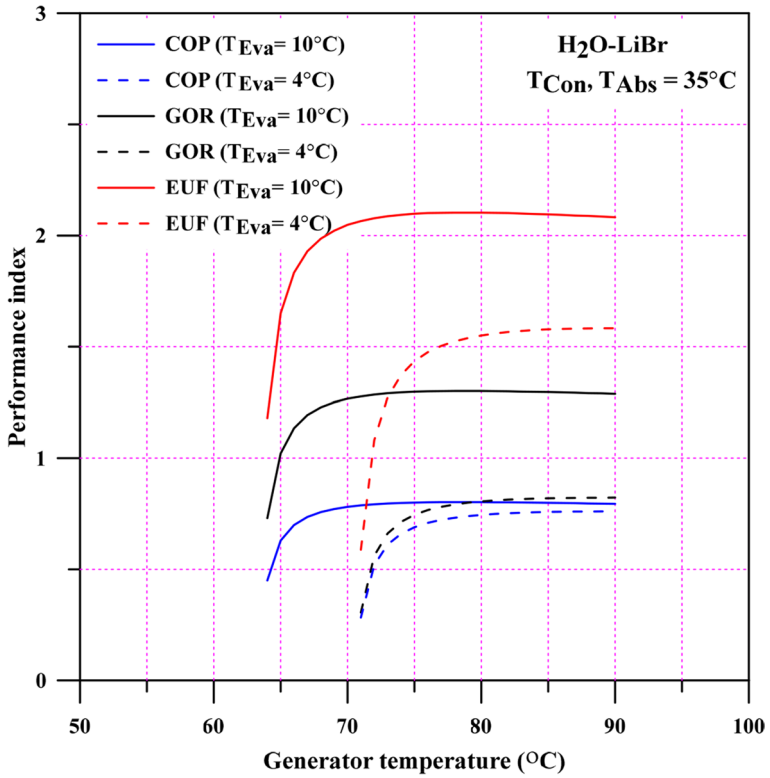

Fig. 5 Variation of performance indexes of hybrid SEAC–HDH with generator temperature at different evaporation temperatures

illustrated below. The total investment cost of the system (Z_{TC}) is defined as the sum of the initial costs (Z_{IC}) of the hole system equipment. That is [23]:

$$Z_{TC} = Z_{IC,cd} + Z_{IC,pf} + Z_{IC,wt} + Z_{IC,pb} + Z_{IC,ac} + Z_{IC,PV} + Z_{IC,d} + Z_{IC,h} + Z_{IC,AB} \quad (7)$$

where the land cost is neglected. The equipment costs appearing in Eq. (6) are given as follows:

Control devices: $Z_{IC,cd} = 80$
Pipes and fittings: $Z_{IC,pf} = 35$
Water tanks: $Z_{IC,wt} = 260$
Pumps and blowers: $Z_{IC,pb} = 345$
Accessories $Z_{IC,ac} = 33$

Dehumidifier

The initial costs of the dehumidifier ($Z_{IC,d}$) for an HDH unit with Ns stages, expressed in terms of the cost of every stage *j* as

$$Z_{IC,d} = \sum_{j=1}^{N_s} Z_{IC,d,j} \quad (8)$$

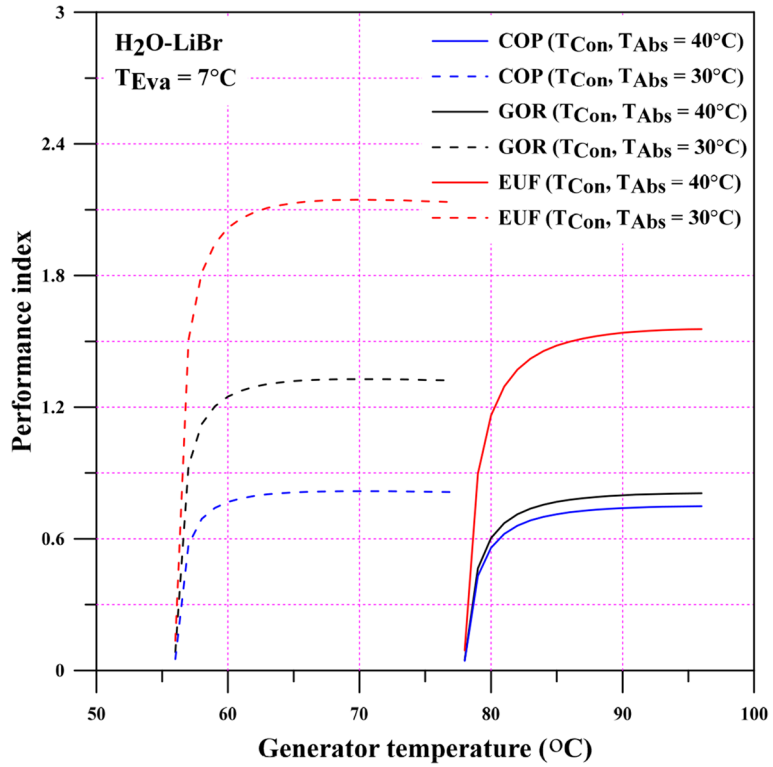

Fig. 6 Dependency of performance indexes of hybrid SEAC–HDH on generator temperature at different condensation temperatures

$$Z_{IC,d,j} = 2143 \times [\frac{\dot{m}_{sw} \times (h_{sw,out} - h_{sw,in})_{d.j}}{U_{d.j}} \times LMTD_{d.j}]]^{0.514} \quad (9)$$

The term $LMTD_{d.j}$ represents the corresponding logarithmic-mean temperature difference, obtained by

$$LMTD_{d.j} = [\frac{\ln[(T_{a,in} - T_{sw,out})/(T_{a,out} - T_{sw,in})]}{(T_{a,in} - T_{sw,out}) - (T_{a,out} - T_{sw,in})}]_{d.j} \quad (10)$$

U_d is the corresponding overall heat transfer coefficient. It is considered fixed at 1400 $W/m^2.K$

Humidifier

The initial costs of the dehumidifier ($Z_{IC,h}$) for an HDH unit with N_s stages, expressed in terms of the cost of every stage *j* as

$$Z_{IC,h} = \sum_{j=1}^{N_s} Z_{IC,h,j} \quad (11)$$

where $Z_{IC,h,j}$ is the humidifier cost of stage *j*. It is estimated by

$$Z_{IC,h,j} = 746.749 \times \left[\dot{m}_{sw,in}^{0.79}\right] \times \left[\frac{(T_{sw,in} - T_{sw,out})^{0.57}}{(T_{sw,in} - T_{a,out})^{0.9942}}[0.022 \times T_{a,out} + 0.39]^{2.447}\right]_{h,j} \quad (12)$$

Flow rates in the above equations are in kg/s, while enthalpies and temperatures are in J/kg and °C, respectively. After calculating Z_{TC}, the annual capital cost of the system ($\dot{Z}_{TC}$) can then be estimated, in $, that is, by multiplying Z_{TC} by the amortization rate (α). It gives,

$$\dot{Z}_{AC} = Z_{AC} \times \alpha \quad (13)$$

$$\alpha = 2143 \times \frac{i \times (i+1)^2}{(i+1)^n - 1} \quad (14)$$

where.

The parameter i above is the interest rate whose value is 5%, The parameter n represents the projected lifetime of the system, and its value is assumed here equal to 20 years. For the annual cost of natural gas ($\dot{Z}_{NG}$), it is estimated by

$$\dot{Z}_{AL} = L_{sc} \times DWP \times f \times 0.001 \times 24 \times 365 \quad (15)$$

where L_{sc} is the specific labor cost. Its value is $0.10 per cubic meter of the desalinated water produced.

Assuming the annual management cost ($\dot{Z}_{AMG}$) to be 20% of $\dot{Z}_{AL}$.

$$\dot{Z}_{AMG} = 0.2 \times \dot{Z}_{AL} \quad (16)$$

Then.

Additionally, the annual maintenance cost ($\dot{Z}_{AM}$) is taken equal to 3% of $\dot{Z}_{AC}$. That is

$$\dot{Z}_{AM} = 0.03 \times \dot{Z}_{AC} \quad (17)$$

$$Z_{ANG} = NG_{uc} \times \frac{1}{293.071} \times \frac{\dot{Q}_{in}}{\eta_{comb}} \times f \times 24 \times 365 \quad (18)$$

The annual cost to be paid for the natural gas consumed ($\dot{Z}_{NG}$) is evaluated by.

Where NG_{uc} is the unit cost of natural gas, taken equal to $4.0/MMBTU [24], and the constant 293.071 shown in Eq. (19) above is for MMBTU-to-kWh unit conversion. Additionally, $\dot{Q}_{in}$ in the above equation must be substituted in kW. Equations (6) to (19) can finally give the desalinated-water specific cost (SCDW) of the proposed system. It is estimated in ¢/l by the following equation:

$$SCDW = \frac{(\dot{Z}_{AC} + \dot{Z}_{ANG} + \dot{Z}_{AL} + \dot{Z}_{AMG}\dot{Z}_{AM}) \times 100}{f \times DWP \times 24 \times 365} \quad (19)$$

The capital investment cost Z˙ ($) of the heat exchangers, pump, valves, humidifier, and dehumidifier are taken from the literature and given in Table 4. Cost values are

Table 4 Capital cost of components of absorption chiller and HDH systems (14)

Component	Capital cost ($)
HPG	$Z_{HPG} = 17,500 \times (\frac{A_{HPG}}{100})^{0.6}$
LPG	$Z_{LPG} = 17,500 \times (\frac{A_{LPG}}{100})^{0.6}$
Condenser	$Z_{Con} = 8,000 \times (\frac{A_{Con}}{100})^{0.6}$
Evaporator	$Z_{Eva} = 16,000 \times (\frac{A_{Eva}}{100})^{0.6}$
Absorber	$Z_{Abs} = 16,500 \times (\frac{A_{Abs}}{100})^{0.6}$
SHE-I	$Z_{SHE-I} = 12,000 \times (\frac{A_{SHE-I}}{100})^{0.6}$
SHE-II	$Z_{SHE-II} = 12,000 \times (\frac{A_{SHE-II}}{100})^{0.6}$
Pump	$Z_{pump} = 1,000 \times (\dot{W}_{pump})^{0.6}$
Valve	$Z_V = 114.5 \times (\dot{m}_V)$
Humidifier	$Z_H = 133$
Dehumidifier	$Z_D = 500$
Fan	$Z_{Fan} = 100$

updated to the present year (2024) according to the Marshall and Swift equipment cost index [25] as

$$\text{Cost of reference year} = \text{present cost} \times \frac{\text{cost index of refence year}}{\text{cost index of presnt year}} \tag{20}$$

Multi-objective optimization

The main objective of this study is to provide a high performance and low cost for the operation of the combined system. Therefore, these two conflicting objectives must be simultaneously optimized which cannot be obtained using the single-objective optimization method. The description of the objective functions and the constraints are as follows:

Optimize: EUF or SCDW

Subjected to

$$60°C \le T_{Gen} \le 105°C;\ 30°C \le T_{Con} \le 40°C;\ 30°C \le T_{Abs} \le 40\ °C; 4°C \le T_{Evap} \le 10°C;\ 0.7 \le \varepsilon_D \le 0.9;\ 0.7 \le \varepsilon_H \le 0.9$$

The influence of the generator temperature (T_{Gen}) on SCDW under different evaporation temperatures and constant condensation temperature is shown in Figs. 7 and 8. As obvious, increasing T_{Eva} or decreasing T_{Con} has a negative impact on the cost of the desalinated water produced by the system. For example, as T_{Eva} increases from 4 to 10 °C, SCDW drops by about 3.68%. The reason behind this impact is that the evaporation temperature has a significant impact on the overall of the combined system. Higher evaporation temperatures allow better heat transfer and evaporation of saline water. This improved in efficiency can result in lower energy consumption and, consequently, reduced costs of desalinated water.

Transient hybrid absorption-HDH system performance

Figure 9 presents the solar irradiance and ambient air temperature for Marsa–Matrouh city hourly all over the year. The maximum ambient air temperature was recorded at

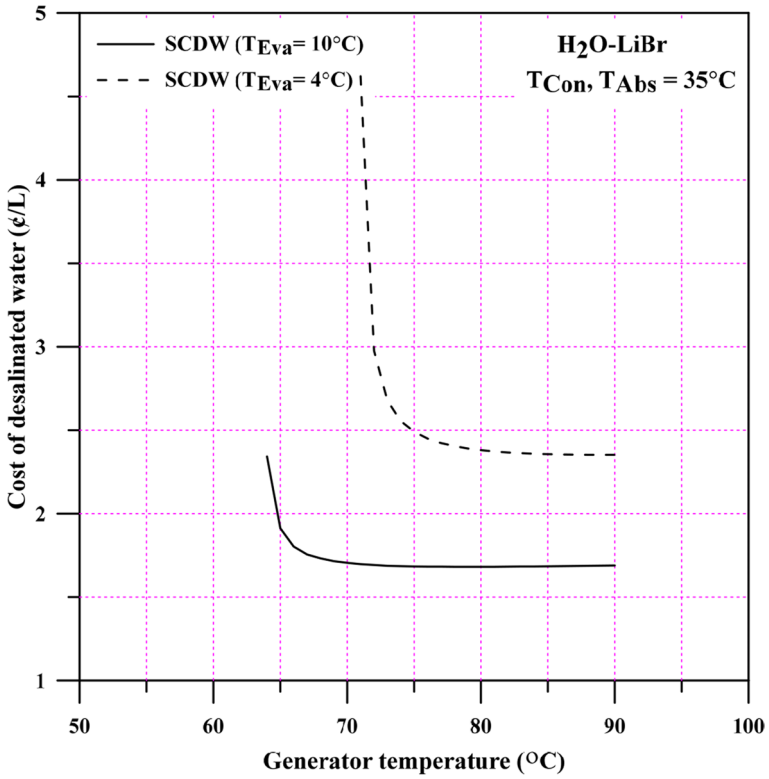

Fig. 7 Variation of SCDW with generator temperature at different evaporation temperatures

33.1 °C on 3rd September and the minimum ambient air temperature was 5.15 °C on 15th January. The maximum solar irradiance is 3.88 kW/m^2 and takes place on 16th October.

Table 5 describes the relationship between the number of collectors and the solar fraction in a solar field system. The solar fraction refers to the percentage of energy that can be supplied by solar energy to the total energy required to drive the system. In general, increasing the number of collectors in a solar system can lead to a higher solar fraction. This is because more collectors can collect a greater amount of solar energy, allowing for more efficient conversion and use of that energy. However, there is a certain number of collectors after this point adding more collectors does not have a significant effect in increasing the solar fraction or energy output. It should be noted that we consider the optimal number of collectors to achieve the desired solar fraction (53 collectors).

Figure 10 shows how applying solar energy affects the hybrid system's GOR and EUF. The use of solar energy on these systems boosted the GOR of the HDH desalination system since solar energy can deliver the required heat at a lower cost than traditional energy sources, resulting in a higher GOR. As illustrated in the figure, the GOR reached 4.3 in June. As a result, the EUF of the hybrid system increased to 7 within the same month. In general, employing solar energy in hybrid absorption cooling and HDH desalination systems can improve GOR and EUF. Solar energy provides a reliable and effective heat source, resulting in increased system efficiency and a lower environmental impact.

The plot in Table 6 shows the extent to which combining the two systems (cooling and desalination) enhances their performance while also reducing the energy required to operate the system. It is obvious that the system performance rose by about three

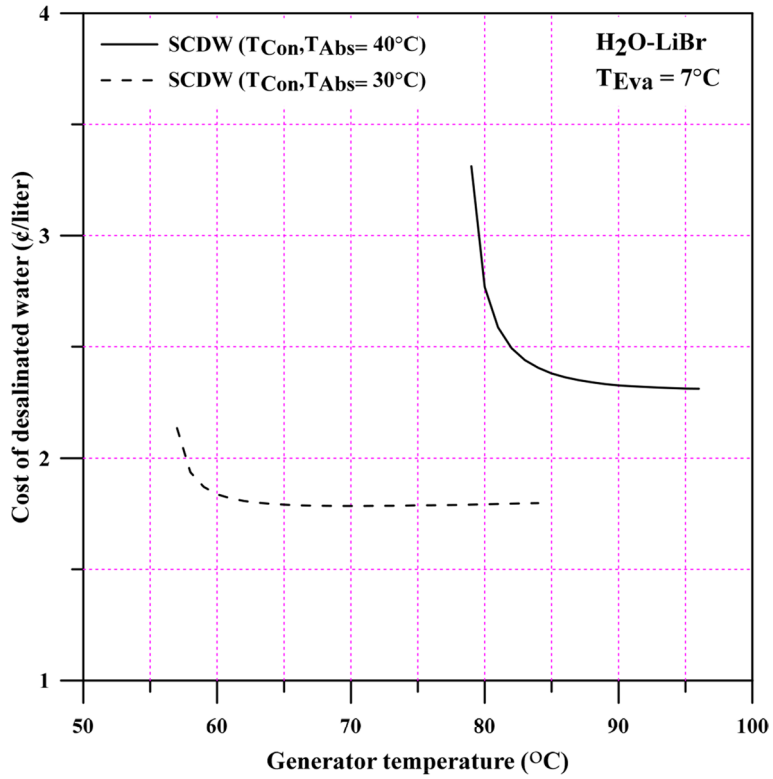

Fig. 8 Reliance of SCDW on generator temperature at different condensation temperatures

times when compared to the individual systems, while the energy required to run the two systems fell by 60%. It also demonstrates the effect of using solar energy as an auxiliary source in significantly increasing the system's performance, up to two times that of the hybrid system without solar energy, and reducing the energy required to half that required in the absence of solar energy.

Multi-objective optimization

The optimization of the combined system is implemented. Six parameters considered for the multi-objective optimization are T_{Gen}, T_{Con}, T_{Abs}, T_{Evap}, ε_D, and ε_H. If the EUF is taken as a single objective function, point A can be treated as the best solution. The point B should be considered if the total product cost of the overall system is taken as a single objective function. Owing to the non-impacting difference in the cost of desalinated water between the two points, therefore, point A (closest point to the ideal point) is selected as the best solution. As the effect of the cost in point B is unobserved about (0.1 Cent/L). The Optimum values of the decision parameters, objective functions, COP, GOR, and flow rate (SCDW) at points A and B are listed in Table 7.

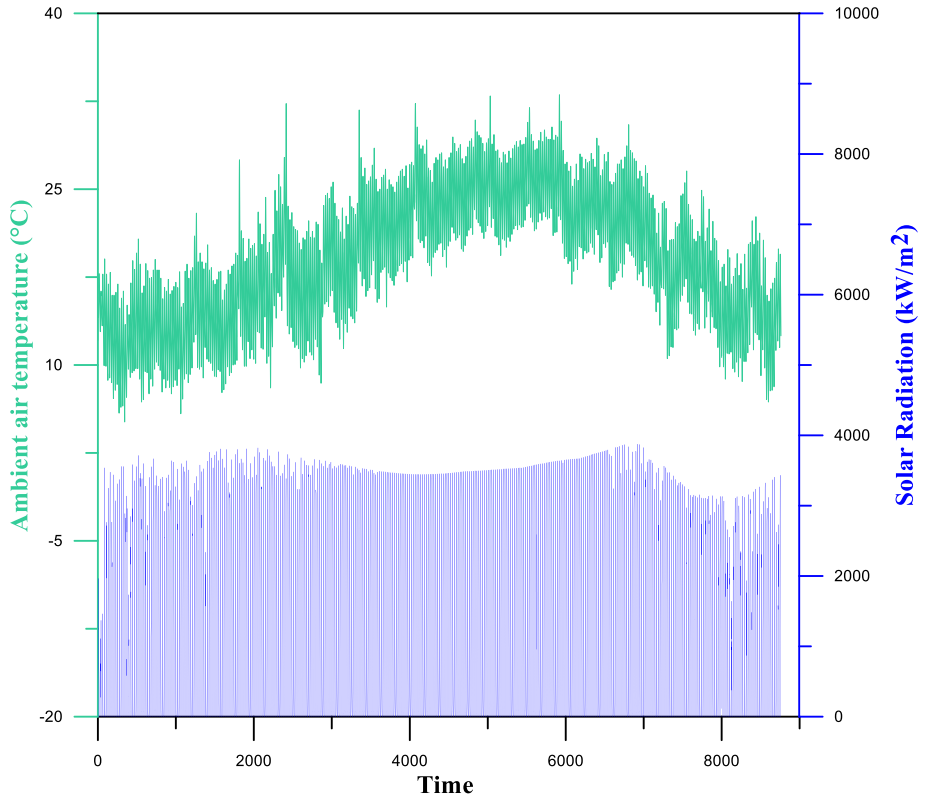

Fig. 9 Marsa-Matrouh weather conditions during simulation time

Table 5 System solar fraction versus collector's number

No of collectors	Solar fraction
0	0
5	0.129
10	0.240
15	0.298
20	0.342
25	0.388
30	0.427
35	0.461
40	0.490
45	0.520
50	0.539
55	0.559
60	0.578
65	0.591
70	0.603
75	0.615
80	0.625
85	0.635

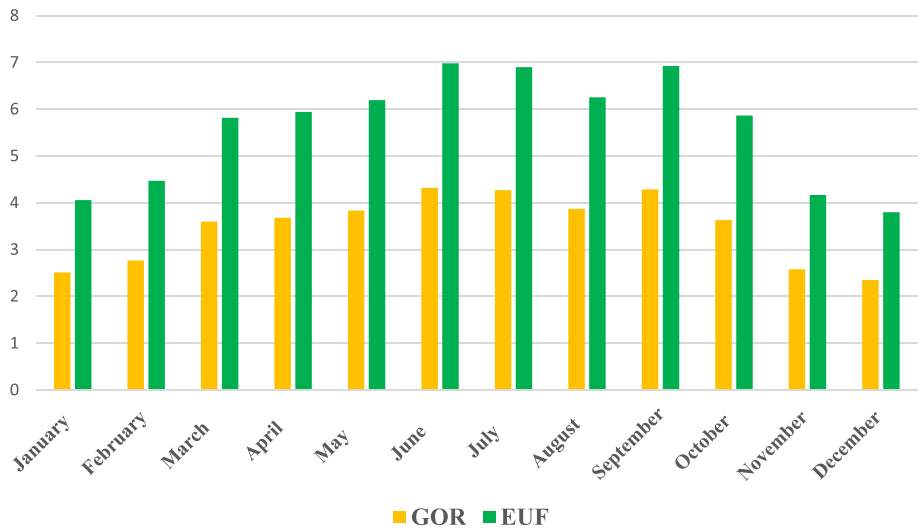

Fig. 10 Monthly system performance indexes

Table 6 Comparison between hybrid and separate systems

	Input energy (kW)	EUF
Separated systems	34.47	0.76
Hybrid system without solar	12.24	2.146
Hybrid system with solar	5.47	4.8

Table 7 Decision parameters and values of objective functions at points A and B

Point	A	B
T_{Gen} (°C)	65	91
T_{Con} (°C)	30	40
T_{Abs} (°C)	30	40
T_{Evap} (°C)	10	10
ε_D	0.9	0.7
ε_H	0.7	0.7
COP	0.8431	0.767
GOR	1.371	1.241
EUF	2.214	2.008
$\dot{m}_{sw}(kg.s^{-1})$	1.491	0.689
SCDW (¢/L)	1.728	1.617

Conclusions

This study looked into a hybrid cooling and desalination system fueled by solar energy. The hybrid system combines a single-effect vapor absorption refrigeration system and a water-heated HDH desalination system. The system has been installed at Marsa-Matrouh, Egypt, with a cooling capacity of 10 kW and freshwater productivity

of 24 L/h. A parametric analysis was performed to explore the impact of operational parameters on system performance indices and to determine the optimal operating conditions, Economic analysis has been studied, and multi-objective optimization is applied to maximize EUF and minimize SCDW. Then, a transient analysis was performed in different climatic circumstances while maintaining the optimal conditions. The most important findings are as follows:

- The maximum hybrid system performance indexes COP, GOR, and EUF are 0.84, 1.37, and 2.21 at the condensation temperature of 30 °C, generation temperature 65 °C, and evaporation temperature of 10 °C.
- The result of the economic analysis of the combined system was calculated as 1.728 Cent/L of desalinated water at optimum operating conditions.
- The proposed system maximum COP, GOR, and EUF increase by 10.4%, 66.3%, and 39.4% as the condensation temperature decreases from 40 to 30 °C at a constant evaporation temperature of 7 °C.
- The optimum hybrid system COP, GOR, and EUF increase by 6.3%, 59.5%, and 34.0% as the evaporation temperature changes from 4 to 10 °C at a constant condensation temperature of 35 °C.
- The proposed hybrid system EUF increases from 0.78 (for separated systems) to 2.15 (for hybrid systems) without solar assistance and can reach 4.8 with the assistance of solar energy. This high rate of increase in system EUF confirms the energy saving for the hybrid systems.
- The system COP as well as the system EUF for the present study is low as the proposed system is a single-stage vapor absorption system integrated with a single-stage HDH. Therefore, an integration of a double-effect absorption system integrated with two-stage HDH can enhance the system performance indexes and achieve lower cooling and water costs.

Abbreviations

AC	Air conditioning
COP	Coefficient of performance
EES	Engineering equation solver
ETC	Evacuated tube collector
EUF	Energy utilization factor
EXP	Expansion valve
GOR	Gained output ratio
HDH	Humidification dehumidification
MR	Mass ratio
SCDW	Specific-cost of desalinated water, ¢/L
SEAC	Single effect absorption cooling
SHE	Solution heat exchanger
TST	Thermal storage tank

Acknowledgements

The used software in this research paper is supported by a research project with the title of "20 Cubic Meter Solar Energy Powered Absorption Cold Store Refrigeration System". The project is funded by STDF (Science & Technology Development Fund) with a project ID.18622.

Authors' contributions

MF was the principal investigator and was responsible for abstracting the study and supervising the overall research direction. EE offered valuable guidance on thermodynamic modeling and helped interpret the results from an energy efficiency perspective. AM provided technical expertise on solar energy integration and system simulations and optimization. NY was the primary researcher, data collection, and analysis. Focused on the design and programming of the hybrid air conditioning system and seawater desalination. All authors revised and contributed to the final manuscript. All authors have read and approved the final manuscript.

Funding
Not applicable.

Availability of data and materials
The datasets used and/or analyzed during the current study are available from the corresponding author on reasonable request.

Declarations

Competing interests
The authors declare that they have no competing interests.

Received: 6 January 2024 Accepted: 20 June 2024
Published online: 06 July 2024

References

1. Kalt G, Wiedenhofer D, Görg C, Haberl H (2019) Conceptualizing energy services: a review of energy and well-being along the Energy Service Cascade. Energy Res Soc Sci 53:47–58
2. IEA International Energy Agency (2023) World energy outlook 2023. https://www.iea.org/reports/world-energy-outlook-2023. Accessed 4 July 2024
3. Wan KKW, Li DHW, Liu D, Lam JC (2011) Future trends of building heating and cooling loads and energy consumption in different climates. Build Environ 46:223–234
4. Nada SA, Elattar HF, Fouda A (2015) Experimental study for hybrid humidification–dehumidification water Desalination and air conditioning system. Desalination 363:112–125
5. UNICEF World Health Organization (2014) Progress on Drinking Water and Sanitation-2014 update. https://data.unicef.org/resources/progress-on-drinking-water-and-sanitation-2014-report/. Accessed 4 July 2024
6. Rijsberman FR (2006) Water scarcity: fact or fiction? Agric Water Manag 80:5–22
7. Chiranjeevi C, Srinivas T (2014) Combined two stage desalination and cooling plant. Desalination 345:56–63
8. Marale S, Chiranjeevi C, Srinivas T, Raj RT (2017) Experimental and computational fluid dynamics studies on dehumidifier in a combined cooling and desalination plant. J Therm Sci Eng Appl 9:011007–011011
9. Nada SA, Fouda A, Mahmoud MA, Elattar HF (2021) Experimental investigation of air-conditioning and HDH desalination hybrid system using new packing pad humidifier and strips-finned helical coil. Appl Therm Eng 185:116433
10. Fouda A, Nada SA, Elattar HF (2016) an integrated A/C and HDH water desalination system assisted by solar energy: transient analysis and economical study. Appl Therm Eng 108:1320–1335
11. He WF, Wen T, Han D, Luo LT, Li RY, Zhong WC (2019) Energetic, entropic and economic analysis of a heat pump coupled humidification dehumidification desalination system using a packed bed dehumidifier. Energy Convers Manage 194:11–21
12. Kabeel AE, Abdelgaied M, Zakaria M (2017) Performance evaluation of a solar energy assisted hybrid desiccant air conditioner integrated with HDH desalination system. Energy Convers Manage 150:382–391
13. Wang N, Wang D, Dong J, Wang H, Wang R, Shao L, Zhu Y (2020) Performance assessment of PCM-based solar energy assisted desiccant air conditioning system combined with a humidification-dehumidification desalination unit. Desalination 496:114705
14. Bhowmick A, Kundu B (2021) Exergoeconomic assessment and optimization of a double effect absorption chiller integrated with a humidification-dehumidification desalination system. Energy Convers Manage 247:114766
15. Beniwal R, Garg K, Tyagi H (2023) Thermodynamics analysis of a novel absorption heat transformer-driven combined refrigeration and desalination system. Energy Convers Manage 277:116597
16. Elgendy E (2024) Energetic performance of a solar driven absorption refrigeration system integrated with humidification dehumidification desalination system. Appl Therm Eng 246:122990
17. Li T, Liu Y, Wang D, Shang K, Liu J (2015) Optimization analysis on storage tank volume in solar heating system. ScienceDirect 121:1356–1364
18. Apricus solar hot water (2016) ETC SOLAR COLLECTOR PRODUCT OVERVIEW. https://rlrnrwxhopim5p.leadongcdn.com/ETC_Collector_Overview_USA-aidlnBqiKipSRromiimlri.pdf. Accessed 4 July 2024
19. Narayan GP, Sharqawy MH, Lienhard JH, Zubair SM (2010) Thermodynamic analysis of humidification dehumanization desalination cycles. Desalination Water Treatment 16:339–353
20. Kaushik SC, Arora A (2009) Energy and exergy analysis of single effect and series flow double effect water–lithium bromide absorption refrigeration systems. Int J Refrig 32:1247–1258
21. Sharqawy MH, Antar MA, Zubair SM, Elbashir AM (2014) Optimum thermal design of humidification dehumidification desalination systems. Desalination 349:10–21
22. Qasem NAA, Zubair SM, Ma AA, Elbassoussi MH (2020) Novel and efficient integration of a humidification-dehumidification desalination system with an absorption refrigeration system. Appl Energy 263:114659
23. Elbassoussi MH, Ahmed MA, Zubair SM, Qasem NAA (2021) On a thermodynamically-balanced humidification-dehumidification desalination system driven by a vapor-absorption heat pump. Energy Convers Manage 238:114142
24. Arhosazani AM, Mohmed WANW (2006) Comparison of Combustion Performance Between Natural Gas And Medium Fuel Oil At Different Firing Settings For Industrial Boilers. In: Proc. International Conference on Energy and Environment (ICEE), Malaysia
25. Economic Indicators (2011) Marshall & Swift equipment cost index. Chem Eng 72